The HKU Scholars Hub   The University of Hong Kong   香港大學學術庫

Title	Solvation and solvent effects on the short-time photodissociation dynamics of CH2I2 from resonance Raman spectroscopy
Author(s)	Kwok, WM; Phillips, DL
Citation	Journal of Chemical Physics, 1996, v. 104 n. 7, p. 2529-2540
Issued Date	1996
URL	http://hdl.handle.net/10722/42341
Rights	Creative Commons: Attribution 3.0 Hong Kong License

Solvation and solvent effects on the short-time photodissociation dynamics of CH_2I_2 from resonance Raman spectroscopy

Wai Ming Kwok and David Lee Phillips
Department of Chemistry, University of Hong Kong, Pokfulam Road, Hong Kong

Resonance Raman spectra of CH_2I_2 have been obtained at excitation wavelengths of 369, 355, and 342 nm in cyclohexane solution and in methanol solution at excitation wavelengths of 355 and 342 nm. Resonance Raman spectra were also measured for CH_2I_2 in the vapor phase with an excitation wavelength of 355 nm. The resonance Raman spectra of CH_2I_2 exhibit most of their intensity in fundamentals, overtones, and combination bands of modes nominally assigned as the I–C–I symmetric stretch, the I–C–I bend, and the I–C–I antisymmetric stretch vibrations. The absorption spectra and resonance Raman intensities of the gas phase and methanol solution phase diiodomethane spectra were simulated using a simple model and time-dependent wave packet calculations. Normal mode coefficients from normal coordinate calculations were used to convert the motion of the wave packet on the excited electronic state surface from dimensionless normal coordinates into internal coordinates of the molecule. The short-time photodissociation dynamics of diiodomethane in the vapor phase shows that the two C–I bonds are lengthening by the same amount, the I–C–I angle becomes smaller, the H–C–I angles become larger, and the H–C–H angle becomes smaller. The two C–I bonds appear essentially equivalent in the Franck–Condon region of the gas phase photodissociation which implies that the molecule chooses which C–I bond is broken after the wave packet has left the Franck–Condon region of the potential energy surface. Comparison of the gas phase resonance Raman spectrum with solution phase spectra obtained in cyclohexane and methanol solvents reveals that the short-time photodissociation dynamics are noticeably changed by solvation with a large solvent-induced symmetry breaking observed. In the Franck–Condon region of the solution phase diiodomethane photodissociation in methanol solvent the two C–I bond become larger by differing amounts, the I–C–I angle becomes smaller, the H–C–H angle becomes smaller, and the H–C–I angles differ from the corresponding gas phase values. During the initial stages of the solution phase photodissociation (at least in methanol and cyclohexane solvents) the two C–I bonds are not the same and this suggests that the molecule chooses which C–I bond will be broken soon after photoexcitation. © *1996 American Institute of Physics.* [S0021-9606(96)01407-X]

I. INTRODUCTION

The time-dependent wave-packet theories of resonance Raman scattering developed by Heller and co-workers[1–3] have made it possible to form an intuitive link between vibrational intensities of the resonance Raman spectra and the short-time dynamics occurring on an excited electronic state potential energy surface. This time-dependent view of the resonance Raman scattering process has led to resonance Raman spectroscopy being used to obtain a large amount of knowledge about the short-time dynamics of photodissociating small polyatomic molecules in the gas phase[4–21] and more recently in liquid solutions.[22–34] Ozone,[4] methyl iodide,[5–9,23–25] iodine,[22,33,34] water,[12,13] NO_2,[10,11] H_2S,[15–17] nitromethane,[18,28] n-propyl iodide,[20] ethyl iodide,[21,26,27] iso-propyl iodide,[21,26,27] tert-butyl iodide,[21,26,27] diiodomethane,[29] chloroiodomethane,[30] bromoiodomethane,[31] and triiodide anion[32] are some of the photodissociating molecules that have been investigated by resonance Raman spectroscopy and interpreted either qualitatively or quantitatively in terms of the time-dependent wave packet picture of resonance Raman scattering.

In this paper, we have chosen to investigate the photo-dissociation dynamics of diiodomethane in both the gas and solution phases. Diiodomethane is a relatively small molecule that can be considered a prototypical molecule for examining photodissociation dynamics of two chromophore systems. Femtosecond time-resolved transient absorption spectroscopy experiments have recently been carried out for diiodomethane in solution by Harris and co-workers.[35] They followed the formation and decay of the CH_2I fragment from the photodissociation of diiodomethane and observed that single collision dominated geminate recombination occurred on the 300–500 fs time scale. The frequency domain resonance Raman spectroscopy experiments and intensity analysis that we report in this paper will complement this time-resolved study by exploring the photodissociation of diiodomethane in the Franck–Condon region before solvent collisions take place ($\lesssim$100 fs). Our study will attempt to probe the vibrational mode-specific dynamics of diiodomethane photodissociation in solution prior to collisions with solvent molecules. We will explore the effects of solvation on the short-time photodissociation dynamics by comparing our solution phase spectra with a gas phase resonance Raman spectrum. We will also search for noticeable solvent

effects on the short-time photodissociation dynamics by comparing resonance Raman spectra obtained in cyclohexane and methanol solvents.

Diiodoalkanes have not been examined in as nearly as much detail[36–44] as monoiodoalkanes. Part of the reason for the relatively few studies on diiodoalkanes are that they contain two C–I chromophores and this makes the absorption spectra and electronic states involved in the photodissociation fairly complicated. The absorption spectrum of the smallest diiodoalkane, diiodomethane, has three broad features that have been deconvoluted into four bands at 214, 249, 285, and 311 nm,[36–38] while the absorption spectrum of the smallest monodiodoalkane, iodomethane, has just one broad band around 260 nm. Photoexcitation of diiodomethane in the ultraviolet leads predominately to breaking one of the C–I bonds to give CH$_2$I radicals and either ground state iodine $^2P_{3/2}$ or electronically excited iodine $^2P_{1/2}$ atoms. It is energetically possible to form CH$_2$ and I$_2$ at wavelengths below 333 nm, but this process is symmetry forbidden.[39,40] Schmitt and Comes[41] carried out flash photolysis experiments and found that formation of CH$_2$ and I$_2$ is at best a minor channel for photoexcitation of diiodomethane in the ultraviolet.

The photodissociation of CH$_2$I$_2$ in the lowest two electronic excited states from 265–340 nm occurs faster than molecular rotation as determined from anisotropy parameters of molecular beam polarization experiments.[36] Translational photofragment spectroscopy experiments[42] determined that the photodissociation of diiodomethane in the A-band absorption leads to CH$_2$I fragments with a large degree of internal excitation and the iodine atoms are formed in the ground or excited electronic states. The vibrational energy distributions of the CH$_2$I photodissociation product at several wavelengths including 248 nm which accesses the next two excited states were found from infrared fluorescence spectroscopy experiments.[43,44] The quantum yield for electronically excited iodine $^2P_{1/2}$ atoms (I*) is usually less than 0.5 and decreases for longer wavelengths.[39] Several research groups have determined the quantum yield of I* formed from photodissociation of CH$_2$I$_2$ excited from 247.5 to 366.5 nm using infrared emission and optoacoustic experiments.[39]

The rest of the paper is structured as follows. The experimental procedure used to obtain the resonance Raman spectra of gas and solution phase diiodomethane is described in Sec. II. The simple model and calculations that were used to simulate the absorption spectra and resonance Raman intensities is presented in Sec. III. The results of the resonance Raman experiments and calculations are presented and discussed in Sec. IV. Comparison of the gas phase with the solution phase results for the short-time photodissociation dynamics of diiodomethane is discussed in Sec. IV D. Finally, Sec. V presents our conclusions about the short-time photodissociation dynamics of diiodomethane in its lowest electronic excited state.

II. EXPERIMENT

CH$_2$I$_2$ (99%), spectroscopic grade cyclohexane (99.9 +%), and spectroscopic grade methanol (99.9+%) (Aldrich) were used as received to prepare samples with concentrations varied from 0.15 to 0.20 M for CH$_2$I$_2$ in cyclohexane and methanol solvents for the resonance Raman experiments. The resonance Raman spectroscopy apparatus has been described previously[29] so we will only give a short description in this section. The third harmonic (355 nm) as well as the Raman shifted lines of the second (369 nm second anti-Stokes) and fourth (342 nm second Stokes) harmonics of a Nd:YAG laser provided the excitation frequencies for the resonance Raman experiments. A backscattering geometry was used to collect the Raman scattered light from the excited region of a flowing liquid stream of CH$_2$I$_2$ sample solution. The Raman scattering was collected by an ellipsoidal mirror with f/1.4 and passed through a polarization scrambler (Oriel) onto the entrance slit of a 0.5 m spectrograph (Acton) with a 1200 groove/mm ruled grating blazed at 250 nm. The grating dispersed the Raman scattering onto a liquid nitrogen cooled CCD detector (Photometrics) mounted on the exit port of the spectrograph. The signal detected by the CCD was collected for about 90 to 600 s before being read out from the CCD detector to an interfaced computer system (PC clone). The resonance Raman spectrum was obtained by summing approximately ten to thirty of these readouts.

The gas phase experiments used the same excitation source, collection optics, and detection equipment as the solution phase experiments. The sample handling apparatus for the gas phase experiments consisted of a heated reservoir of liquid and vapor diiodomethane connected to a heated pipette. Dry nitrogen was passed though the sample reservoir to carry away some of the diiodomethane vapor with it through the pipette nozzle. The excitation laser beam was loosely focused near the exit of the pipette nozzle and an approximate 90° geometry was used. The laser power was kept relatively low ($\sim$100 μj over a 2 mm beam diameter) to avoid interference from photoproduct peaks which were readily observable at much higher powers (1 mj and higher in a 1 mm beam diameter). The 355 nm light was not noticeably attenuated by the vapor phase sample and reabsorption of the resonance Raman scattering was minimal for the gas phase experiments.

Known Raman frequencies of cyclohexane or methanol solvent lines (solution phase spectra) and mercury emission lines as well as gas phase nitrogen and oxygen peaks (for the gas phase spectrum) were used to calibrate the wavenumber Raman shifts of the resonance Raman spectra. The backscattering light collection geometry used in the solution phase experiments helps to minimize the reabsorption of the Raman scattered light by the sample. The methods described in Ref. 45 were used to correct the solution phase spectra for the remaining reabsorption of the Raman scattered light by the sample. The solvent peaks were removed from the reabsorption corrected spectra by subtracting an appropriately scaled solvent spectrum. The channel to channel variation of the whole detection system as a function of wavelength was taken into account by taking a spectrum of a calibrated intensity standard D$_2$ lamp (Optronics) and/or a calibrated intensity standard tungsten lamp (Optronics). Regions of the corrected spectra were fitted to a base line plus a sum of

Lorentzians to find the integrated areas of the Raman peaks.

III. THEORY AND CALCULATIONS

We have chosen to use a relatively simple model to simulate the resonance Raman intensities to determine the major differences between the gas and solution phase photodissociation dynamics of diiodomethane. This simple model and calculations will also provide a reference to which more sophisticated calculations can be compared to help assess the importance of various effects or processes such as thermally populated modes, possible Duschinsky rotation of normal modes, coordinate dependence of the transition moment, coupling to solvent motions, and others. The model and calculations presented here are not meant to be a complete description of the resonance Raman and absorption spectra data, but serve as a guide to elucidate the major differences between the gas and solution phase spectra and short-time photodissociation dynamics.

Heller's time-dependent wave packet approach to resonance Raman scattering similar to those applied in Refs. 26 and 28 was used to simulate the resonance Raman intensities and the first excited electronic state of diiodomethane. The absorption spectrum is calculated from

$$\sigma_A(E_L) = (4\pi e^2 E_L M^2/3n\hbar^2 c)$$
$$\times \mathrm{Re} \int_0^\infty \langle 0|0(t)\rangle \exp[i(E_L+\epsilon_i)t/\hbar] \qquad (1)$$

and the resonance Raman cross sections are calculated using

$$\sigma_{R,0-f}(E_L) = (8\pi e^4 E_S^3 E_L M^4/9\hbar^6 c^4)$$
$$\times \left| \int_0^\infty \langle f|0(t)\rangle \exp[i(E_L+\epsilon_i)t/\hbar] \right|^2, \qquad (2)$$

where E_L is the incident photon energy, E_S is the scattered photon energy, n is the solvent index of refraction, M is the transition length evaluated at the equilibrium geometry, $|0(t)\rangle = e^{-iHt/\hbar}|0\rangle$ which is $|0(t)\rangle$ propagated on the excited state surface for a time t, H is the excited state vibrational Hamiltonian, and f is the final state for the resonance Raman process. We have used the Gaussian deconvolution of the experimental absorption spectrum to help guide the determination of the calculation parameters for fitting the A-state absorption spectrum of diiodomethane.

Harmonic oscillators with their potential minima separated by Δ in dimensionless normal coordinates were used to approximate the ground and excited state potential energy surfaces. This bound harmonic oscillator model for the excited state potential energy surface only provides a convenient way to mimic the portion of the excited state surface in the Franck–Condon region that determines the resonance Raman intensities and absorption spectrum and does not suggest that the excited state is actually bound. The harmonic oscillators were allowed to have either the same frequencies or different frequencies as appropriate. The calculations include no Duchinsky rotation of the normal coordinates and the transition moment M includes no coordinate dependence. The multidimensional overlaps in Eqs. (1) and (2) then become products of one-dimensional harmonic oscillator overlaps. Thermal population of initial states other than $|0(t)\rangle$ was ignored for the Raman active normal modes although the ν_4 (I–C–I bend) vibrational mode has significant population in states higher than $v=0$ at room temperature. The time integrals in Eqs. (1) and (2) were truncated after the wave packet had initially moved far from the origin so as to have no significant overlap for any of the final states seen in our Raman spectrum. This truncation of the time integrals was used in place of an explicit damping function that represents the effects of excited state population decay and/or electronic pure dephasing and has been discussed previously for directly photodissociating molecules in Refs. 26 and 28. The absence of any vibrational structure in the experimental gas and solution phase absorption spectra of CH₂I₂ suggests that the total electronic dephasing is dominated by dissociation prior to the first vibrational recurrence.

Dimensionless normal coordinates are generally used in describing the potential parameters used in Eqs. (1) and (2). In order to easily visualize the short-time photodissociation dynamics in terms of bond length and bond angle changes, the normal coordinate motions were converted into internal coordinate motions in the following manner. The center of the wave packet at time t after excitation to the electronic excited state and undergoing separable harmonic dynamics can be described in dimensionless normal coordinates by

$$q_\alpha(t) = \Delta_\alpha(1 - \cos \omega_\alpha t), \qquad (3)$$

where the vibrational frequency, ω_α, is in units of fs⁻¹, the time, t, is in units of fs and we fix $q_\alpha=0$ for each mode α at the ground electronic state equilibrium geometry. The internal coordinate displacements at different times t are then found from the dimensionless normal mode displacements, $q_\alpha(t)$, by the following equation:

$$s_i(t) = (h/2\pi c)^{1/2} \sum_\alpha A_{\alpha i} \varpi_\alpha^{-1/2} q_\alpha(t), \qquad (4)$$

where s_i are the displacements of the internal coordinates (bond stretches, bends, torsions, and wags as defined by Wilson, Decius, and Cross) from their ground electronic state equilibrium values, $A_{\alpha i}$ is the normal-mode coefficient $(\partial s_i/\partial Q_\alpha)$, Q_α is the ordinary dimensioned normal coordinate, and ϖ_α is the vibrational frequency in units of cm⁻¹. An adapted version of the Snyder and Schachtschneider FG program (described in detail in Ref. 46) was used to compute the normal-mode vectors diiodomethane. Previously published ground-state geometries and valence force fields[47] were used to calculate the normal mode vibrational frequencies and normal mode coefficients for diiodomethane. The force field gave a rms frequency error of 4.36 cm⁻¹ for the nine normal mode vibrations of diiodomethane. Table I presents the calculated and experimental[47] frequencies for the nine normal modes of diiodomethane. The complete force field, Cartesian coordinates, computed vibrational frequencies, and normal-mode coefficients are available as supplementary material.[47]
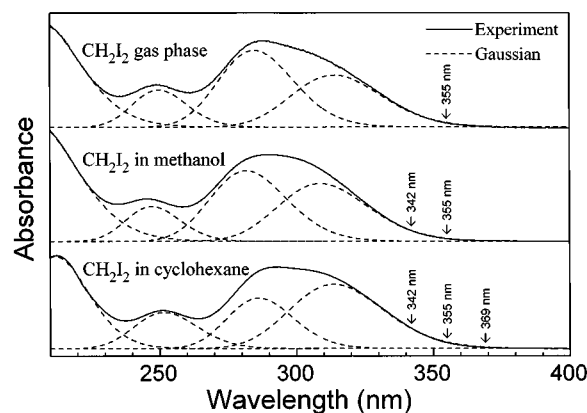
FIG. 1. Diiodomethane absorption spectra in the gas phase, in cyclohexane solution, and in methanol solution. The excitation wavelengths for the resonance Raman experiments are shown by the arrows and numbers (in nm) above each absorption spectrum. The dashed lines in the absorption spectra are four Gaussian peaks used to fit the absorption. The 342, 355, and 369 nm excitation wavelengths are in resonance with the lowest excited electronic state of diiodomethane.

IV. RESULTS AND DISCUSSION

A. Absorption spectra

Figure 1 displays the absorption spectra of diiodomethane in the gas phase, in cyclohexane solvent and in methanol solvent. The excitation wavelengths for the resonance Raman spectra are shown as arrows and wavelengths in nm above the absorption spectra. The dashed lines in Fig. 1 for the absorption spectra present the four Gaussian peaks we are able to fit to each experimental absorption spectrum. The absorption spectra of diiodomethane we obtain are in general agreement with those previously published by several groups.[14,36–38,44] The absorption spectrum of diiodomethane was deconvoluted into a sum of four Gaussian bands by Baughcum and Leone[44] and Zhang and Imre[14] and our present deconvolution of the absorption bands are very similar to theirs. Excitation within the lowest excited electronic state centered ~32 000 cm⁻¹ forms only ground elec-

tronic state iodine atoms, while excitation within the second and higher electronic states leads to production of both ground and excited electronic states of iodine. We plan to investigate the short-time photodissociation dynamics of the second excited-state of diiodomethane and this will be reported in the future.[48] However, the present paper focuses on the short-time photodissociation dynamics of the first excited state of diiodomethane which forms only ground electronic state iodine atoms. We have selected excitation wavelengths of 341.5 and 355 nm in order to examine the first electronic state without significant excitation into other higher energy excited electronic states.[39]

B. Resonance Raman spectra

Figure 2 shows the resonance Raman spectrum of gas phase diiodomethane taken with 355 nm excitation. Most of the larger Raman peaks in the spectrum are labeled and have been tentatively assigned based on the previously reported 355 nm gas phase resonance Raman spectrum of Zhang and Imre[14] and a preresonance 436 nm Raman spectrum of neat liquid diiodomethane.[37] The overall intensity pattern of our gas phase spectrum agrees fairly well with that obtained by

TABLE I. Diiodomethane ground state normal modes.

Mode	Experimental frequency (cm⁻¹)	Calculated frequency (cm⁻¹)
ν_1	2968	2967
ν_2	1351	1347
ν_3	486	486
ν_4	121	127
ν_5	1028	1022
ν_6	3049	3050
ν_7	716	719
ν_8	1105	1112
ν_9	570	568

TABLE II. Comparison of experimental and calculated 355 nm resonance Raman intensities of vapor phase diiodomethane.

Peak	Raman shift[a] (cm⁻¹)	Experiment intensity[b]	Calculated intensity[c]
ν_3	499	699	256
$2\nu_3$	979	100	100
$3\nu_3$	1454	61	47
$4\nu_3$	1937	14	25
$\nu_3 - \nu_4$	382	28	
$\nu_3 + \nu_4$	604	40	39
$2\nu_3 + \nu_4$	1094	22	29
$2\nu_9$	1158	60	56
$2\nu_9 + \nu_3$	1639	35	41
$2\nu_9 + 2\nu_3$	2119	19	26
$2\nu_9 + \nu_3 + \nu_4$	1747	9	10
ν_2	1379	21	21

[a]Estimated uncertainties are about 8 cm⁻¹ for the Raman shifts.
[b]Relative intensities are based on integrated areas of the peaks. Estimated uncertainties are about 10% for intensities 50 and higher, 15% for intensities between 15 and 50, and 30% for intensities lower than 15.
[c]The resonance Raman intensities were calculated using the parameters of Table V in Eq. (2) and the model described in Sec. III.
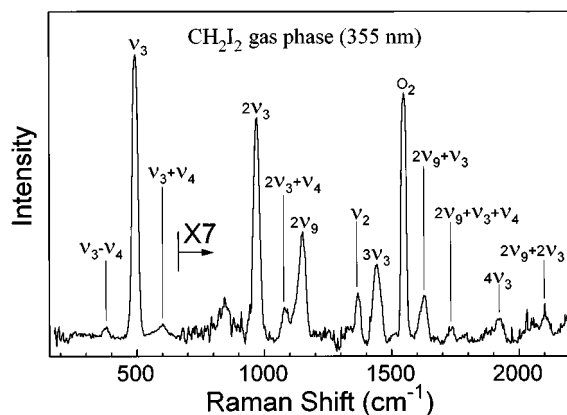

FIG. 2. Resonance Raman spectrum of gas phase diiodomethane obtained with 355 nm excitation. The spectrum intensities have been intensity corrected. The assignments of the larger Raman bands are labeled.
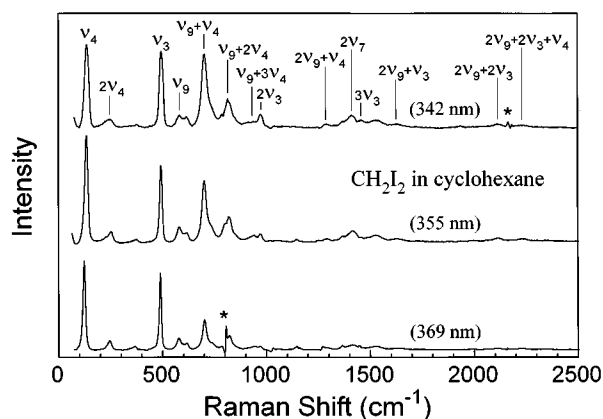
FIG. 3. Resonance Raman spectra of diiodomethane in cyclohexane solution obtained with 342, 355, and 369 nm excitation wavelengths. These spectra have been intensity corrected and solvent subtracted. The assignments of the larger Raman peaks have been labeled. These spectra were taken with excitation within the lowest excited electronic state of diiodomethane. The asterisks mark regions with solvent subtraction artifacts.

TABLE III. Experimental resonance Raman intensities for diiodomethane in cyclohexane solution at excitation wavelengths of 342 and 355 nm.

Peak	Raman shift[a] (cm^{-1})	342 nm intensity[b]	355 nm intensity[b]
ν_4	134	814	1510
$2\nu_4$	243	143	260
$\nu_3-\nu_4$	372	41	60
ν_3	493	677	1000
$2\nu_3$	973	100	100
$3\nu_3$	1459	62	
$4\nu_3$	1938	45	
$\nu_3+\nu_4$	614	87	140
ν_9	581	133	310
$\nu_9+\nu_4$	703	819	1680
$\nu_9+2\nu_4$	815	436[c]	1200[c]
$\nu_9+3\nu_4$	933	118	240
$2\nu_9$	1145		40
$2\nu_9+\nu_4$	1291	41	160
$2\nu_9+\nu_3$	1632	89	210
$2\nu_9+\nu_3+\nu_4$	1731	26	60
$2\nu_9+2\nu_3$	2110	126	300
$2\nu_9+2\nu_3+\nu_4$	2231	122	250
$2\nu_9+2\nu_3+2\nu_4$	2352		140
ν_2	1369	114	110
$2\nu_7$	1415	168	700
$2\nu_7+\nu_9$	1994		70
$2\nu_9+\nu_3-\nu_4$ and $2\nu_7+\nu_4$	1527	250	590

[a]Estimated uncertainties are about 4 cm^{-1} for the Raman shifts.
[b]Relative intensities are based on integrated areas of the peaks. Estimated uncertainties are about 10% for intensities 500 and higher, 15% for intensities between 150 and 500, and 30% for intensities lower than 150.
[c]Estimated uncertainty is approximately 30% due to solvent subtraction.

Zhang and Imre.[14] Fundamentals, overtones, and/or combination bands of three Franck–Condon active modes ν_4 (I–C–I bend), ν_3 (I–C–I symmetric stretch), and ν_9 (I–C–I antisymmetric stretch) account for the majority of the Raman intensity in our gas phase spectrum. We observe several overtones ($2\nu_3$, $3\nu_3$, $4\nu_3$, and $2\nu_9$) and combination bands ($2\nu_9+\nu_3$ and $2\nu_9+2\nu_3$) that were also observed in the gas phase spectrum of Zhang and Imre.[14] Since our gas phase spectrum has higher signal to noise, this allows us to observe several Raman peaks not seen before. In particular, our gas phase spectrum has significant combination bands of ν_4 with ν_3 and $2\nu_9$ ($\nu_3-\nu_4$, $\nu_3+\nu_4$, $2\nu_3+\nu_4$, and $2\nu_9+\nu_3+\nu_4$) that were either not assigned or not observed in the previously reported gas phase spectrum. The Raman peak positions and relative intensities of the gas phase 355 nm resonance Raman spectrum of Fig. 2 are shown in Table II.

Figure 3 displays the 342, 355, and 369 nm resonance Raman spectra of diiodomethane in cyclohexane solution. The larger Raman peaks are labeled in Fig. 3 and the peak positions and relative intensities are listed in Table III for the 342 and 355 nm spectra. We see overtones of four Franck–Condon active modes ($2\nu_3$, $3\nu_3$, $4\nu_3$, $2\nu_4$, $2\nu_9$, and $2\nu_7$) as well as many combination bands of these vibrational modes ($\nu_3-\nu_4$, $\nu_3+\nu_4$, $\nu_9+\nu_4$, $\nu_9+2\nu_4$, $\nu_9+3\nu_4$, $2\nu_9+\nu_4$, $2\nu_9+\nu_3$, $2\nu_9+2\nu_3$, $2\nu_9+2\nu_3+\nu_4$, and $2\nu_9+2\nu_3+2\nu_4$). Comparison of the diiodomethane in cyclohexane solution resonance Raman spectra with the gas phase spectrum shows there are significant differences between the solution phase and gas phase, particularly in the following peaks: $\nu_9+\nu_4$, $\nu_9+2\nu_4$, $\nu_9+3\nu_4$, $2\nu_7$, $2\nu_9+2\nu_3+\nu_4$, and $2\nu_9+2\nu_3+2\nu_4$. We will discuss the differences between the solution and gas phase spectra more fully in Sec. IV D.

Figure 4 shows the resonance Raman spectra of diiodomethane in methanol solvent taken with excitation wavelengths of 355 and 342 nm. The larger peaks in the spectra are labeled and the relative intensities (342 nm) as well as peak positions are reported in Table IV. We observe

overtones of three Franck–Condon active vibrational modes ($2\nu_3$, $3\nu_3$, $4\nu_3$, $2\nu_4$, and $2\nu_9$) and several combination bands of these modes ($\nu_3-\nu_4$, $\nu_3+\nu_4$, $\nu_9+\nu_4$, $\nu_9+2\nu_4$, $2\nu_9+\nu_3$, and $2\nu_9+2\nu_3$).

The resonance Raman spectra of Figs. 2, 3, and 4 show some general trends in their resonance Raman intensity pat-
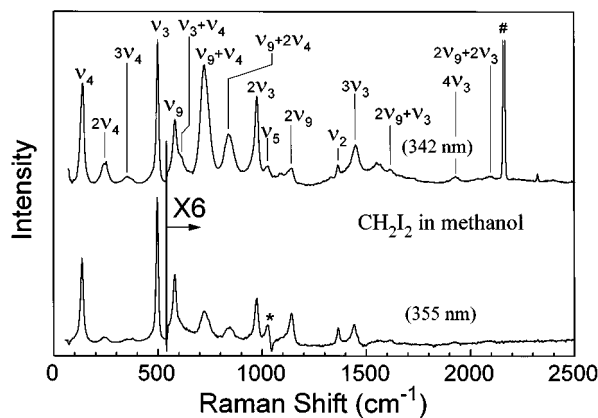

FIG. 4. Resonance Raman spectra of diiodomethane in methanol solution obtained with 342 and 355 nm excitation wavelengths. These spectra have been intensity corrected and solvent subtracted. The assignments of the larger Raman peaks have been labeled. These spectra were taken with excitation within the lowest excited electronic state of diiodomethane. The asterisk marks a solvent subtraction artifact and the pound sign (#) marks a laser line artifact.

TABLE IV. Comparison of experimental and calculated 342 nm resonance Raman intensities of diiodomethane in methanol solution.

Peak	Raman shift[a] (cm^{-1})	Experiment intensity[b]	Calculated intensity[c]
ν_3	501	614	481
$2\nu_3$	980	100	100
$3\nu_3$	1454	84	24
$4\nu_3$	1941	13	6
ν_4	141	730	741
$2\nu_4$	248	270	232
$3\nu_4$	354	87	88
$\nu_3-\nu_4$	381	16	
$\nu_3+\nu_4$	613	24	317
ν_9	585	74	437
$\nu_9+\nu_4$	730	286	268
$\nu_9+2\nu_4$	849	113	143
$2\nu_9$	1145	19	39
$2\nu_9+\nu_3$	1630	20	30
$2\nu_9+2\nu_3$	2102	6	15
ν_5	1032	14	14
ν_2	1379	19	19

[a]Estimated uncertainties are about 4 cm^{-1} for the Raman shifts.
[b]Relative intensities are based on integrated areas of the peaks. Estimated uncertainties are about 10% for intensities 50 and higher, 15% for intensities between 15 and 50, and 30% for intensities lower than 15.
[c]The resonance Raman intensities were calculated using the parameters of Table V in Eq. (2) and the model described in Sec. III.

terns. The gas phase spectrum of Fig. 2 has the simplest pattern with only a few important overtone and combination band progressions. The resonance Raman spectra of Fig. 4 for diiodomethane in methanol solvent have more resonantly enhanced peaks than the gas phase spectrum of Fig. 2 but fewer resonantly enhanced peaks than the spectra of diiodomethane in cyclohexane in Fig. 3. The intensity of the $\nu_9, \nu_9+\nu_4, \nu_9+2\nu_4$ peaks are stronger in cyclohexane than in methanol and are not observed in the gas phase spectrum.

C. Simulations of absorption spectra and resonance Raman intensities

Our approach to modeling the absorption and resonance Raman spectra differs from the approach previously applied to gas phase diiodomethane photodissociation dynamics by Zhang, Heller, Huber, Imre, and Tannor[49] who constructed model potential energy surfaces based on information known for the single chromophore iodomethane. Their model fixed the I–C–I bond angle at 110° for the calculations and no attempt was made to model the I–C–I bending motion. The model of Zhang, Heller, Huber, Imre, and Tannor[49] used two Franck–Condon active modes, the nominal symmetric I–C–I stretch (ν_3) and the nominal I–C–I antisymmetric stretch (ν_9), and fit the experimental data of Zhang and Imre well for the four largest overtones and combination bands observed in the gas phase spectrum ($2\nu_3$, $3\nu_3$, $2\nu_9$, and $2\nu_9+\nu_3$).[14]

Our gas phase diiodomethane spectrum (Fig. 2) shows several new combination bands ($\nu_3-\nu_4$, $\nu_3+\nu_4$, $2\nu_3+\nu_4$, and $2\nu_9+\nu_3+\nu_4$.) either not reported or not assigned by Zhang and Imre. These bands indicate that we should not ignore the

contributions of the nominal I–C–I bend vibrational mode modes (ν_4) in simulating our resonance Raman spectra. Our solution phase resonance Raman spectra show substantial intensity in overtones of ν_4 and combination bands of ν_4 (nominal I–C–I bend) with other vibrational modes. In order to make comparisons between the gas and solution phase short-time photodissociation dynamics we have used a simple model described in Sec. III that includes the nominal I–C–I bending vibrational mode (ν_4).

The parameters listed in Table V were used in Eqs. (1) and (2) to calculate the gas phase absorption spectrum and 355 nm resonance Raman intensities of diiodomethane. Figure 5 shows the comparison of the experimental and calculated absorption spectrum along with the first Gaussian peak from deconvolution of the experimental absorption spectrum. Figure 6 displays the comparison of 355 nm experimental and calculated resonance Raman intensities for gas phase diiodomethane. Table II compares the experimental and calculated resonance Raman intensities for gas phase diiodomethane with 355 nm excitation. The calculated absorption spectrum is broad and fits the red edge of the first absorption band and the Gaussian deconvolution of the experimental absorption spectrum reasonably well. Inspection of Fig. 6 shows that the calculated resonance Raman intensities generally agree well with the experimental intensities with only a couple of exceptions: the fundamental of the I–C–I symmetric stretch (ν_3) is calculated to be over 3 times to small compared to the experimental intensity and the calculated intensity of our relatively simple model does not give any intensity to the $\nu_3-\nu_4$ difference band since we have not thermally populated the overtone of the I–C–I bending mode (ν_4). Improving our simple model to include thermally populated vibrational modes (in particular, the low frequency I–C–I bending mode) will most likely allow us to better fit the difference band intensity and a calculation with thermally populated vibrational modes will be reported in the future. We note that the model and calculations of Ref. 49 also calculated a ν_3 fundamental intensity that was far to low compared to the experimental intensity. It is not too surprising that we have difficulty fitting the intensity of the fundamental of the I–C–I symmetric stretch (ν_3) since fundamental resonance Raman intensities are often prone to interference effects from contributions to the fundamental intensity from other nearby electronic states and care must be taken in the interpretation of fundamental intensities. This has been observed for several alkyl iodide A-band resonance Raman spectra.[7,25,26]

It is not clear whether ν_2 (CH$_2$ scissor) is actually Franck–Condon active in the lowest excited electronic state of diiodomethane since we only observe its fundamental and do not observe significant intensity in overtones and/or combination bands. Nevertheless, the ν_2 (CH$_2$ scissor) vibrational mode was included in the calculation for completeness to fit the fundamental intensity that appears in the 355 nm gas phase resonance Raman spectrum. The calculations with and without this mode present do not change significantly since this mode only makes a very weak contribution to the overall resonance Raman intensity and absorption spectrum.

TABLE V. Parameters for calculation of resonance Raman intensities and absorption spectrum of vapor phase diodomethane and diiodomethane in methanol solution.

Vibrational mode	Ground state vibrational frequency (cm^{-1})	Excited state vibrational frequency (cm^{-1})	$|\Delta|$
A. Vapor Phase Diiodomethane			
ν_4 (I–C–I bend)	134 cm^{-1a}	134 cm^{-1}	5.6
ν_3 (I–C–I symmetric stretch)	499 cm^{-1}	499 cm^{-1}	4.0
ν_9 (I–C–I antisymmetric stretch)	581 cm^{-1}	−770 cm^{-1}	0.00
ν_2 (CH$_2$ scissor)	1379 cm^{-1}	1379 cm^{-1}	0.56
Transition length, M =0.197 Å E_0=25 700 cm^{-1}			
B. Diiodomethane in Methanol Solution			
ν_4 (I–C–I bend)	141 cm^{-1}	180 cm^{-1}	5.9
ν_3 (I–C–I symmetric stretch)	501 cm^{-1}	501 cm^{-1}	2.4
ν_9 (I–C–I antisymmetric stretch)	585 cm^{-1}	780 cm^{-1}	1.3
ν_5 (CH$_2$ twist)	1032 cm^{-1}	1032 cm^{-1}	0.24
ν_2 (CH$_2$ scissor)	1375 cm^{-1}	1375 cm^{-1}	0.24
Transition length, M =0.256 Å E_0=25 800 cm^{-1}			

[a]Value of fundamental vibrational frequency estimated from our resonance Raman spectra.

The other three vibrational modes [ν_4 (I–C–I bend), ν_3 (I–C–I symmetric stretch), and ν_9 (I–C–I antisymmetric stretch)] are most likely Franck–Condon active in the first excited electronic state of gas phase diiodomethane since overtones and/or combination bands have significant intensity and they are much less likely to have interference or large contributions from nonresonant electronic states because overtones and combination band intensities decrease faster far from resonance than fundamental intensities. Most of the short-time photodissociation dynamics of gas phase diiodomethane can be described in terms of these three Franck–Condon active vibrational motions.

Examination of Table V shows that the two totally symmetric modes [ν_4 (I–C–I bend) and ν_3 (I–C–I symmetric stretch)] have relatively large normal mode displacements with magnitudes of 5.6 and 4.0, respectively. It may seem somewhat surprising that the low frequency ν_4 (I–C–I bend) mode has such a large normal mode displacement in the first excited state although its combination bands with other modes are relatively weak [$\nu_3-\nu_4$, $\nu_3+\nu_4$, $2\nu_3+\nu_4$, $2\nu_9+\nu_4$, and $2\nu_9+2\nu_3+\nu_4$] compared to the overtone and combination band intensities associated with the ν_3 (I–C–I symmetric stretch) mode as shown in Table II. This effect is the result of short-time dynamics associated with the direct photodissociation of diiodomethane and the multidimensional
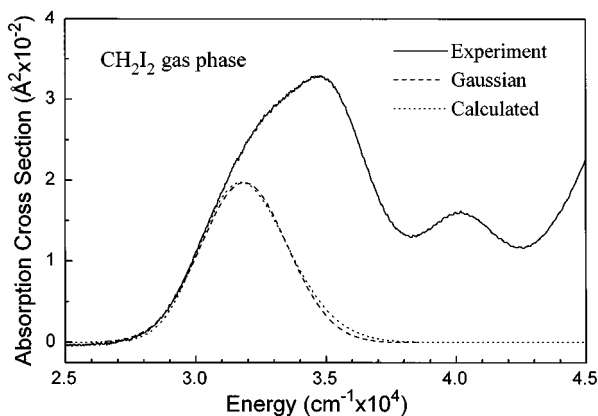

FIG. 5. Comparison of experimental (solid line) and calculated (dotted line) absorption spectra of gas phase diiodomethane as well as the Gaussian peak (dashed line) of the A state from deconvolution of the experimental spectrum. The calculated absorption spectrum made use of the parameters of Table V in Eq. (1) and the model described in Sec. III.
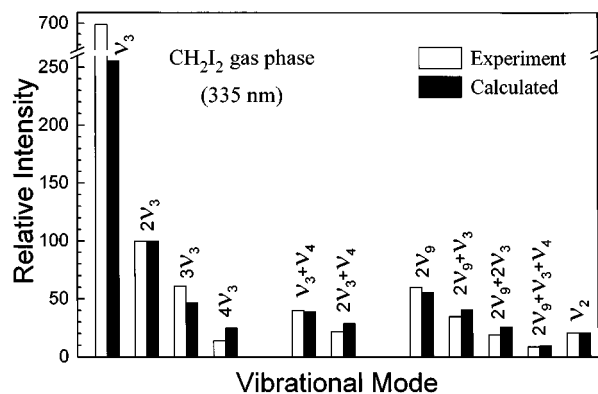

FIG. 6. Comparison of experimental (open bars) and calculated (solid black bars) resonance Raman intensities for the 355 nm resonance Raman spectrum of gas phase diiodomethane. The calculated resonance Raman intensities made use of the parameters of Table V in Eq. (2) and the model described in Sec. III.

nature of the dissociation. When there is no fast damping mechanism such as direct photodissociation or multimode effects, then the time-averaged single-mode Raman overlap $\langle f|i(t)\rangle$ for modes with the same normal mode displacement $|\Delta|$ will have about the same Raman intensity averaged over the excitation profile for the absorption band. However, fast processes that quickly move the wave packet out of the Franck–Condon region will damp the Raman overlaps and result in lower absolute Raman cross sections compared to the case where these fast processes do not occur. Two fast processes that will rapidly damp the Raman overlaps for our gas phase diiodomethane resonance Raman intensities are the direct photodissociation that moves the initially excited wave packet out of the Franck–Condon region and the multidimensional nature of the photodissociation that quickly moves the initially excited wave packet along several different vibrational modes. The vibrational mode frequency affects the time scale of vibrational oscillations with lower frequency modes taking longer to reach their first maximum. The longer time to reach their first maximum for lower frequency vibrational modes results in lower frequency vibration Raman overlaps to be damped much more quickly than higher frequency vibration Raman overlaps. Thus, a low frequency vibration needs to have a larger $|\Delta|$ to have about the same amount of intensity as a higher frequency vibration. In our case a relatively large $|\Delta|$ is needed for the low frequency ν_4 (I–C–I bend) mode to closely fit the observed intensity in the $\nu_3+\nu_4$, $2\nu_3+\nu_4$, and $2\nu_9+\nu_3+\nu_4$ combination bands.

The large normal mode displacements, $|\Delta|$, for both the ν_4 (I–C–I bend) and ν_3 (I–C–I symmetric stretch) modes implies that the short-time photodissociation of gas phase diiodomethane has a noticeable change in the I–C–I bond angle and in the bond lengths of the two C–I bonds. Electronic excitation transfers electron density from the nonbonding lone-pair-like orbitals on the iodine atoms to the C–I antibonding σ^* orbitals and this gives a node in the electronic wavefunction between the two C–I bonds.[14,36] This node will keep the two iodine atoms from coming too close together to form an iodine molecule from direct photodissociation of diiodomethane which is consistent with the observation of Schmitt and Comes[41] that any I$_2$ photoproduct formed is at best a minor photodissociation channel for ultraviolet wavelengths. The node in the excited electronic state could cause the two iodine atoms to separate farther apart and give rise to I–C–I bending motion during the short-time photodissociation dynamics. However, if the photodissociation pushes the carbon atom away from each very massive iodine atoms similar to the short-time photodissociation dynamics found in iodoethane, 2-iodopropane, and tert-butyl iodide for the C–C–I bond angles then we could expect that the I–C–I angle will decrease.[26] Either of these cases is consistent with the large normal mode displacement, $|\Delta|$, for the ν_4 (I–C–I bend) vibration we use to model the $\nu_3+\nu_4$, $2\nu_3+\nu_4$, and $2\nu_9+\nu_3+\nu_4$ combination band intensities. Electronic excitation of diiodomethane is also known to result in one of the C–I bonds being broken to give CH$_2$I and I fragments. This is consistent with the large normal mode displacement $|\Delta|$, for the ν_3 (I–C–I symmetric stretch) vibra-

tion we use to model the $2\nu_3$, $3\nu_3$, and $4\nu_3$ overtone intensities.

The third large Franck–Condon active mode, ν_9 (I–C–I antisymmetric stretch), is a nontotally symmetric mode and its fundamental and odd quanta are not observed in the gas phase resonance Raman spectrum due to symmetry constraints. However, the overtone of the I–C–I antisymmetric stretch and its combination bands with other modes are present ($2\nu_9$, $2\nu_9+\nu_3$, and $2\nu_9+2\nu_3$) in the gas phase diiodomethane resonance Raman spectrum. We needed a large frequency change from 581 cm^{-1} in the ground electronic state to -770 cm^{-1} (a locally unbound potential with the imaginary frequency represented by a negative number) in the excited electronic state to fit the large amount of intensity in the overtone of the I–C–I antisymmetric stretch and its combination bands ($2\nu_9$, $2\nu_9+\nu_3$, and $2\nu_9+2\nu_3$). We also had to set $|\Delta|=0.0$ to obtained no intensity in the ν_9 (I–C–I antisymmetric stretch) fundamental and its combination bands with other modes that do not appear in our gas phase resonance Raman spectrum. This would indicate that there is predominately spreading of the wave packet along the I–C–I antisymmetric stretch coordinate in the excited state with no significant displacement of the center of the wave packet along the I–C–I symmetric stretch in the Franck–Condon region.

In order to easily visualize the short-time photodissociation dynamics of diiodomethane we will use the results of our modeling and normal mode calculations in Eqs. (3) and (4) to find the internal coordinates as a function of time. To make use of Eqs. (3) and (4) we need to know the signs of the normal mode displacements since the resonance Raman intensity analysis only provides us the magnitude of the normal mode displacements. Determining the sign of the normal mode displacements, $|\Delta|$, can be done in several ways. For some cases one can try to assume that the normal modes are pure internal coordinates, but this is usually not a good approximation and is definitely not applicable to diiodomethane where the normal mode descriptions of the three important Franck–Condon active modes show significant contributions from several different internal coordinates. It is possible to solve the sign problem of the normal mode displacements by using resonance Raman intensity data for several different isotopic derivatives and finding the geometry change(s) with least variance across the set of isotopic derivatives. Another way to help find the signs of the normal mode displacements is to use the results of electronic structure and/or chemical intuition to eliminate many possible sign combinations of the normal coordinate displacements. This is the approach we will use for diiodomethane. For a more thorough discussion of the problem of choosing the signs of the normal coordinate displacements the reader is referred to several recent review articles dealing with resonance Raman intensity analysis.[50,51]

Since we know that one of the C–I bonds is broken in a direct photodissociation, we will assume that the C–I bond(s) become longer upon excitation. This gives us a negative sign for the normal mode displacement for the I–C–I symmetric stretch mode and either a positive or negative

TABLE VI. Most probable internal coordinate displacements of diiodomethane at $t=15$ fs assuming the C–I bond becomes longer.

Internal coordinate	Gas phase 15 fs[a]	Solution phase (in methanol solvent)	
		15 fs with $\Delta_9=+1.3$[b]	15 fs with $\Delta_9=-1.3$[c]
C–H bonds	−0.008 Å	−0.004 Å	−0.004 Å
	(−0.009 Å)	(−0.006 Å)	(−0.006 Å)
C–I bond, atoms 1 and 4	+0.146 Å	+0.169 Å	+0.010 Å
	(+0.142 Å)	(+0.162 Å)	(+0.004 Å)
C–I bond, atoms 1 and 5	+0.146 Å	+0.010 Å	+0.169 Å
	(+0.142 Å)	(+0.004 Å)	(+0.162 Å)
H–C–H angle, atoms 2, 1, and 3	−2.4°	−1.5°	−1.5°
	(−2.5°)	(−1.4°)	(−1.4°)
H–C–I angle, atoms 2, 1, and 4	+2.8°	−0.4°	+3.5°
	(+3.2°)	(+0.1°)	(+4.0°)
H–C–I angle, atoms 3, 1, and 5	+2.8°	+3.5°	−0.4°
	(+3.2°)	(+4.0°)	(+0.1°)
H–C–I angle, atoms 2, 1, and 5	+2.9°	+3.5°	−0.2°
	(+3.3°)	(+4.0°)	(+0.3°)
H–C–I angle, atoms 3, 1, and 4	+2.9°	−0.2°	+3.5°
	(+3.3°)	(+0.3°)	(+4.0°)
I–C–I angle, atoms 4, 1, and 5	−8.9°	−4.9°	−4.9°
	(−11°)	(−7.0°)	(−7.0°)

[a]Values without parentheses are for the sign combination of $\Delta_3=-4.0$ and $\Delta_4=+5.6$, while values within parentheses are for the sign combination of $\Delta_3=-4.0$ and $\Delta_4=-5.6$.
[b]Values without parentheses are for the sign combination of $\Delta_3=-2.4$, $\Delta_4=+5.9$, and $\Delta_9=+1.3$ while values within parentheses are for the sign combination of $\Delta_3=-2.4$ and $\Delta_4=-5.9$, and $\Delta_9=+1.3$.
[c]Values without parentheses are for the sign combination of $\Delta_3=-4.0$, $\Delta_4=+5.9$, and $\Delta_9=-1.3$ while values within parentheses are for the sign combination of $\Delta_3=-4.0$ and $\Delta_4=-5.9$, and $\Delta_9=-1.3$.

normal mode displacement for the I–C–I symmetric bend mode. The I–C–I antisymmetric stretch normal mode displacement is zero and it is neither positive or negative. Using the basic assumption that the C–I bond(s) become longer we can use the results of our normal coordinate calculations and Eqs. 3 and 4 to find the internal coordinates as a function of time. Table VI shows the internal coordinate changes for gas phase diiodomethane at 15 fs assuming that the C–I bond length increases. We chose a time of 15 fs because the calculated $\langle f|i(t)\rangle$ overlaps that determine the resonance Raman intensities reach their maxima between 10 and 20 fs for most of the observed Raman peaks and is short compared to the vibrational recurrence times of any of the three important Franck–Condon active modes. We note that we have used harmonic potentials to mimic a much more complicated dissociative potential energy surface, so we can only reasonably talk about the short-time photodissociation dynamics where the nuclei have not moved too far away from the Franck–Condon region.

The short-time photodissociation dynamics implied by the results in Table VI show that gas phase diiodomethane stretches both C–I bonds by a large amount equally, the I–C–I angle becomes smaller, the H–C–H angle become smaller, and the H–C–I angles become larger. The short-time dynamics are similar to that of a "soft radical" model[52] of photodissociation dynamics in which the carbon atom is pushed into the rest of the radical as the C–I bond becomes longer. This "soft radical" photodissociation would then predict the I–C–I angle becomes smaller, the H–C–I angle becomes larger and the H–C–H angle becomes larger. The

short-time photodissociation dynamics we see in Table VI agree qualitatively with the "soft-radical" description except for the change in the H–C–H angle which becomes smaller instead of larger as predicted by the "soft radical" picture. We are not very sensitive to C–H or H–C–H motions in our resonance Raman intensity analysis since the higher frequency modes are not Franck–Condon active and apparently are not strongly coupled to the initial stages of the photodissociation. The main reason that we see the H–C–H angle change in the short-time dynamics is due to the H–C–H bend contribution to the normal mode of the I–C–I symmetric stretch vibration. Thus, the changes in the H–C–H angle comes about primarily from Franck–Condon excitation of the I–C–I symmetric stretch normal coordinate and not direct excitation of a mode that has primarily an H–C–H bend vibration.

D. Solvation and solvent effects: Comparison of gas and solution phase resonance Raman spectra

Examination of the resonance Raman spectra of gas phase and solution phase diiodomethane in Figs. 2–4 show some striking differences in the overall intensity patterns, particularly for the I–C–I antisymmetric stretch fundamental and combination bands with the I–C–I bending mode. The antisymmetric stretch I–C–I vibrational mode is a nontotally symmetric mode whose fundamental and combination bands with the totally symmetric I–C–I bending mode (ν_9, $\nu_9+\nu_4$, $\nu_9+2\nu_4$, and $\nu_9+3\nu_4$) should not be present in the resonance Raman spectra if the molecule has a strict C_{2v} symmetry.

The symmetry restrictions hold for gas phase diiodomethane and these peaks (ν_9, $\nu_9+\nu_4$, $\nu_9+2\nu_4$, and $\nu_9+3\nu_4$) are not present in the gas phase spectrum of Fig. 2. The two C–I bonds in the gas phase diiodomethane molecules are essentially identical since the molecules are very far apart from one another and interact very weakly. Thus, for gas phase diiodomethane we would expect that the C_{2v} symmetry restriction would hold very well. The gas phase short-time photodissociation dynamics (discussed in Section IV C) makes no real distinction between the two C–I bonds and does not choose which C–I bond will be broken until the wave packet has moved some distance along the reaction coordinate.

When diiodomethane is taken from the relatively isolated molecule environment of the gas phase and is dissolved in liquid solvents, the photodissociation dynamics becomes more complicated. Examination of Table V shows that the normal mode displacement for ν_3 (I–C–I symmetric stretch) is 2.4 for diiodomethane in methanol solution which is reduced from the corresponding value of 4.0 for gas phase diiodomethane. This reduction is probably expected since the intensity of the ν_3 (I–C–I symmetric stretch) overtone progression relative to other intensities in the resonance Raman spectra decrease in the diiodomethane in methanol solution spectra compared to the gas phase spectra. The solvent perturbations at any one time will not likely affect each C–I bond equally since the configuration of solvent molecules around each C–I bond will most likely not be the same. These solvent perturbations can reduce the symmetry of the diiodomethane molecule and allow nontotally symmetric vibrational modes such as the I–C–I antisymmetric stretch fundamental (ν_9) and its combination bands with the I–C–I bending mode (ν_4) to become Raman active also ($\nu_9+\nu_4$, $\nu_9+2\nu_4$, $\nu_9+3\nu_4$). The amount of symmetry breaking is very solvent dependent with the symmetry breaking stronger in cyclohexane than in methanol solution. The observed solvent-induced symmetry-breaking may be due primarily to mode-specific solvent-solute interactions and/or a polarization solvent-solute interaction. The time scale of solvent fluctuations relative to the resonance Raman scattering time scale will most likely also play a role in the amount of symmetry breaking observed in different solvents. For example, the solvent fluctuations may be faster in methanol than in cyclohexane solution so that symmetry of the two C–I chromophores is better maintained in methanol than in cyclohexane leading to less symmetry breaking in methanol than in cyclohexane. We plan to further investigate the mechanism of this large symmetry breaking by examining resonance Raman spectra of diiodomethane in large variety of solvents with different properties and this will be reported at a later time.[53]

For the methanol solution resonance Raman intensities we needed a frequency change from 585 cm^{-1} in the ground electronic state to 780 cm^{-1} in the excited electronic state to fit the amount of intensity in the overtone of the I–C–I antisymmetric stretch and its combination bands ($2\nu_9$, $2\nu_9+\nu_3$, and $2\nu_9+2\nu_3$). We also had to set $|\Delta|=1.3$ to obtain enough intensity in the ν_9 (I–C–I antisymmetric stretch) plus ν_4 (I–

C–I bend) combination bands ($\nu_9+\nu_4$ and $\nu_9+2\nu_4$). We could not fit the ratio of the odd combination bands ($\nu_9+\nu_4$, and $\nu_9+2\nu_4$) to the overtone and its combination bands ($2\nu_9$, $2\nu_9+\nu_3$, and $2\nu_9+2\nu_3$) very well using a locally unbound potential with an imaginary frequency as in the gas phase simulations. Furthermore, we were unable to closely fit the shape of the first Gaussian peak of the deconvolution (representing the first excited state of diiodomethane) of the experimental absorption spectrum using a frequency much higher than 780 cm^{-1} (for example an 1100 cm^{-1} frequency gave a calculated absorption spectrum that was noticeably too broad). Our model does not necessarily imply that the I–C–I antisymmetric stretch coordinate is bound in solution. The portion of the excited state surface that determines the resonance Raman intensities for the first few overtones and/or combination bands is the slope of the excited state when no recurrences take place. We note that the displacement of 1.3 is fairly large and the Raman overlaps corresponding to the odd combination bands ($\nu_9+\nu_4$ and $\nu_9+2\nu_4$) to the overtone and its combination bands ($2\nu_9$, $2\nu_9+\nu_3$, and $2\nu_9+2\nu_3$) approach zero by the time the integral is truncated. Thus the solution phase parameters of Table V are consistent with mimicing a locally unbound repulsive excited state along the nominal I–C–I antisymmetric stretch with one C–I bond preferentially lengthened over the other C–I bond.

Table VI shows the most probable internal coordinate displacements at $t=15$ fs assuming the C–I bond lengths increase for diiodomethane in the gas phase and methanol solution and Fig. 9 shows the geometry of CH$_2$I$_2$. Inspection of Table VI reveals that the reduction of symmetry caused by solvent molecule perturbations leads to one C–I bond being lengthened faster than the other C–I bond. Both C–I bonds appear to be affected by the nearby solvent molecules during the initial stages of photodissociation. Examination of Table VI reveals that most of the internal coordinate displacements of solution phase diiodomethane are noticeably different (by varying degrees) than their corresponding gas phase values. This appears to indicate that the motions of the short-time photodissociation are influenced by the presence of nearby solvent molecules even before there are any full collisions on average with a solvent molecule. Closer examination of Table VI shows that the difference between the gas phase and solution phase (methanol solution) internal coordinate displacements during the initial stages of photodissociation depend strongly on which particular internal coordinate is involved.

One of the most interesting features of the short-time photodissociation dynamics is that the configuration of solvent molecules about diiodomethane in methanol solution appears to inhibit one C–I bond from lengthening as much as the other C–I bond. The molecule seems to choose which C–I bond to break early in the photodissociation in the solution phase (i.e., in the Franck–Condon region) while the molecule appears to choose which C–I bond will break later in the photodissociation in the gas phase (i.e., outside the Franck–Condon region). The reduction of symmetry in the solution phase resonance Raman spectra of diiodomethane could be considered a result of how the presence of solvent
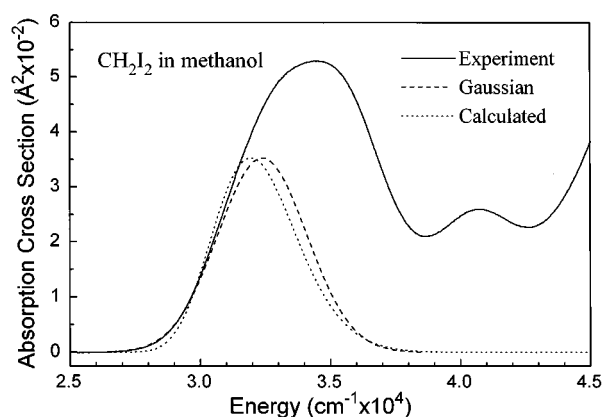
FIG. 7. Comparison of experimental (solid line) and calculated (dotted line) absorption spectra of diiodomethane in methanol solution as well as the Gaussian peak (dashed line) of the *A* state from deconvolution of the experimental spectrum. The calculated absorption spectrum made use of the parameters of Table V in Eq. (1) and the model described in Sec. III.
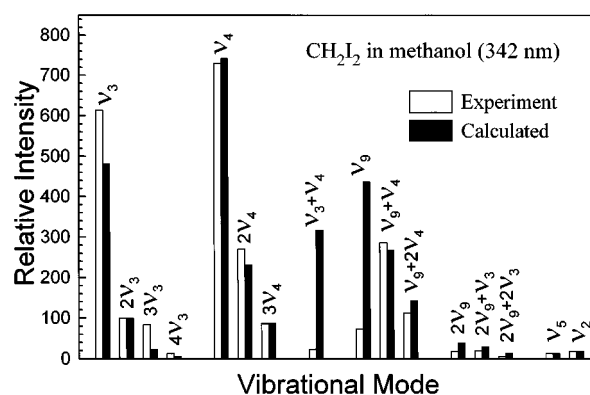

FIG. 8. Comparison of experimental (open bars) and calculated (solid black bars) resonance Raman intensities for the 342 nm resonance Raman spectrum of diiodomethane in methanol solution. The calculated resonance Raman intensities made use of the parameters of Table V in Eq. (2) and the model described in Sec. III.

molecules modify the short-time photodissociation dynamics of diiodomethane.

We should note a few caveats at this point. Our simulations of the resonance Raman intensities and absorption spectra make several approximations (such as only $v=0$ modes are initially populated, the Condon approximation, and no Duchinsky rotation of normal modes) which can be improved to provide more accurate and quantitative short-time photodissociation dynamics. The simple simulations that we report with our experimental data serve as a semi-quantitative guide to the major features of the short-time photodissociation dynamics of diiodomethane in the gas phase and in methanol solution. These calculations also point out the major differences between the gas phase and solution phase short-time photodissociation dynamics. The choice of the signs of the normal mode displacements is based on the assumption that the C–I bonds become longer in the excited state relative to the ground state geometry which is probably a good assumption since one of the C–I bonds will be broken in this direct photodissociation. The description of the normal coordinates was based on a previously published force field[47] for diiodomethane and this only compared experimental and calculated vibrational frequencies for fully protonated diiodomethane. The force field could probably be refined further by comparing experimental and calculated vibrational frequencies for several isotopic derivatives (CH$_2$I$_2$, CD$_2$I$_2$, and CHDI$_2$, for example). An improvement in the description of the normal modes would also help to obtain more accurate short-time photodissociation dynamics in terms of the internal coordinates. While our very simple model (described in Sec. III) does a fairly good job of fitting both the absorption band and resonance Raman intensities in the gas phase, this model does not do as well for the methanol solution data (compare Figs. 5–8 and Tables II and IV). It is possible that dynamic solvent effects such as a changing excited state potential with motion of the solvent molecules during the initial stages of the photodissociation may be

needed to better simulate the solution phase resonance Raman and absorption spectra.

V. CONCLUSION

We have reported resonance Raman spectra of diiodomethane obtained with excitation in its lowest electronic excited state for the gas phase, in methanol solution and in cyclohexane solution. These spectra are dominated by fundamentals, combination bands, and overtones of three Franck–Condon active vibrational modes: ν_4 (I–C–I bend), ν_3 (I–C–I symmetric stretch), and ν_9 (I–C–I antisymmetric stretch). We have used a simple model and time-dependent wave packet calculations to simulate the resonance Raman intensities and the absorption spectrum for gas phase diiodomethane and diiodomethane in methanol solution. The results of these calculations were used in conjunction with the description of the normal mode vibrations to determine the short-time photodissociation dynamics of diiodomethane
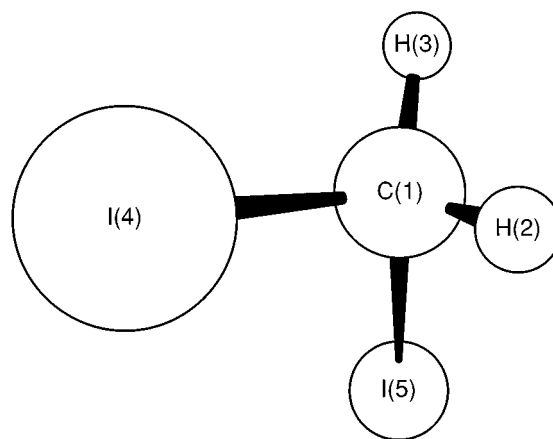

FIG. 9. Geometry of diiodomethane used in the normal coordinate calculations. All C–H bond lengths are 1.093 Å, all C–I bond lengths are 2.1195 Å, and all bond angles are 109.45°. Each atom is labeled with a number 1 through 5.

in terms of easy to visualize internal coordinate motions. During the initial stages of the photodissociation of gas phase diiodomethane, the two C–I bonds are lengthened by the same amount, the I–C–I angle becomes smaller, the H–C–I angles become larger, and the H–C–H angle becomes smaller. The two C–I bonds are essentially equivalent in the gas phase photodissociation in the Franck–Condon region and this indicates that the molecule chooses which C–I bond is broken after both C–I bonds have been stretched considerably and after the wave packet has left the Franck–Condon region. Solvation significantly modifies the short-time photodissociation dynamics of diiodomethane. During the short-time photodissociation of diiodomethane in methanol solution, the two C–I bonds become longer by different amounts in contrast to the same C–I bond lengthening observed in the gas phase. The two C–I bonds are not equivalent in the solution phase photodissociation in the Franck–Condon region and this probably indicates that the molecule chooses which C–I bond is broken soon after photoexcitation. Solvation also appears to inhibit the motion of the molecule with the magnitudes of the internal coordinate motions generally reduced (although not always) relative to their gas phase values due to solvent-solute interactions. We also note the significant differences in the relative intensity patterns of the resonance Raman spectra obtained in methanol solution and cyclohexane solution which indicate that solvent-solute interactions depend strongly on the nature of the solvent.

Future work will involve developing better models and calculations for describing the resonance Raman spectral intensities and absorption spectra. Further experiments[53] are in progress to probe the nature of the solvent-solute interaction that appears to have a strong solvent dependence on the short-time photodissociation dynamics of diiodomethane in the solution phase.

ACKNOWLEDGMENTS

[1] E. J. Heller J. Chem. Phys. **62**, 1544 (1975).

[2] S. Y. Lee and E. J. Heller, J. Chem. Phys. **71**, 4777 (1979).

[3] E. J. Heller, R. L. Sundberg, and D. J. Tannor, J. Phys. Chem. **86**, 1822 (1982).

[4] D. G. Imre, J. L. Kinsey, R. W. Field, and D. H. Katayama, J. Phys. Chem. **86**, 1822 (1982).

[5] D. G. Imre, J. L. Kinsey, A. Sinha, and J. Krenos, J. Phys. Chem. **88**, 3956 (1984).

[6] M. O. Hale, G. E. Galica, S. G. Glogover, and J. L. Kinsey, J. Phys. Chem. **90**, 4997 (1986).

[7] G. E. Galica, B. R. Johnson, J. L. Kinsey, and M. O. Hale, J. Phys. Chem. **95**, 7994 (1991).

[8] K. Q. Lao, M. D. Person, P. Xayaroboun, and L. J. Butler, J. Chem. Phys. **92**, 823 (1990).

[9] P. G. Wang and L. D. Zeigler, J. Phys. Chem. **97**, 3139 (1993).

[10] E. A. Rolfing and J. J. Valentini, Chem. Phys. Lett. **114**, 282 (1985).

[11] E. A. Rolfing and J. J. Valentini, J. Chem. Phys. **83**, 521 (1985).

[12] R. J. Sension, R. J. Brudzynski, and B. S. Hudson, Phys. Rev. Lett. **61**, 694 (1988).

[13] R. J. Sension, R. J. Brudzynski, B. S. Hudson, J. Z. Zhang, and D. G. Imre, Chem. Phys. **141**, 393 (1990).

[14] J. Zhang and D. G. Imre, J. Chem. Phys. **89**, 309 (1988).

[15] K. Klienermans, E. Linnebach, and R. J. Suntz, J. Phys. Chem. **91**, 5543 (1987).

[16] M. D. Person, K. Q. Lao, B. J. Eckholm, and L. J. Butler, J. Chem. Phys. **91**, 812 (1989).

[17] R. J. Brudzynski, R. J. Sension, and B. S. Hudson, Chem. Phys. Lett. **165**, 487 (1990).

[18] K. Q. Lao, E. Jensen, P. W. Kash, and L. J. Butler, J. Chem. Phys. **93**, 3958 (1990).

[19] P. W. Browning, E. Jensen, G. C. G. Waschewsky, M. R. Tate, L. J. Butler, and J. P. Hessler, J. Chem. Phys. **101**, 5652 (1994).

[20] D. L. Phillips, B. A. Lawrence, and J. J. Valentini, J. Phys. Chem. **95**, 7570 (1991).

[21] D. L. Phillips, B. A. Lawrence, and J. J. Valentini, J. Phys. Chem. **95**, 9085 (1991).

[22] R. J. Sension and H. L. Strauss, J. Chem. Phys. **85**, 3791 (1986).

[23] F. Markel and A. B. Myers, Chem. Phys. Lett. **167**, 175 (1990).

[24] A. B. Myers and F. Markel, Chem. Phys. **149**, 21 (1990).

[25] F. Markel and A. B. Myers, J. Chem. Phys. **98**, 21 (1993).

[26] D. L. Phillips and A. B. Myers, J. Chem. Phys. **95**, 226 (1991).

[27] D. L. Phillips, J. J. Valentini, and A. B. Myers, J. Phys. Chem. **96**, 2039 (1992).

[28] D. L. Phillips and A. B. Myers, J. Chem. Phys. **95**, 7164 (1991).

[29] W. M. Kwok and D. L. Phillips, Chem. Phys. Lett. **235**, 260 (1995).

[30] D. L. Phillips and W. M. Kwok, Chem. Phys. Lett. **241**, 267 (1995).

[31] S. Q. Man, W. M. Kwok, and D. L. Phillips, J. Phys. Chem. **99**, 15 705 (1995).

[32] A. E. Johnson and A. B. Myers, J. Chem. Phys. **102**, 3519 (1995).

[33] J. Xu, N. Schwentner, and M. Chergui, J. Chem. Phys. **101**, 7381 (1994).

[34] J. Xu, N. Schwentner, S. Hennig, and M. Chergui, J. Chim. Phys. **92**, 541 (1995).

[35] B. J. Schwartz, J. C. King, J. Z. Zhang, and C. B. Harris, Chem. Phys. Lett. **203**, 503 (1993).

[36] M. Kawasaki, S. J. Lee, and R. Bersohn, J. Chem. Phys. **63**, 809 (1975).

[37] C. Fotakis, M. Martin, and R. J. Donovan, J. Chem. Soc. Faraday Trans. II **78**, 1363 (1982).

[38] A. Gedanken and M. D. Rowe, Chem. Phys. **36**, 181 (1979).

[39] J. B. Koffend and S. R. Leone, Chem. Phys. Lett. **81**, 136 (1981).

[40] S. R. Cain, R. Hoffman, and R. Grant, J. Phys. Chem. **85**, 4046 (1981).

[41] G. Schmitt and F. J. Comes, J. Photochem. **14**, 107 (1980).

[42] P. M. Kroger, P. C. Demou, and S. J. Riley, J. Chem. Phys. **65**, 1823 (1976).

[43] S. L. Baughcum, H. Hofmann, S. R. Leone, and D. J. Nesbitt, Faraday Discuss. Chem. Soc. **67**, 306 (1979).

[44] S. L. Baughcum and S. R. Leone, J. Chem. Phys. **72**, 6531 (1980).

[45] A. B. Myers, B. Li, and X. Ci, J. Chem. Phys. **89**, 1876 (1988).

[46] B. U. Curry, Ph.D. dissertation, University of California, Berkeley, 1983.

[47] F. L. Voelz, F. F. Cleveland, A. G. Meister, and R. B. Bernstein, J. Opt. Soc. Am. B **43**, 1061 (1953). See AIP document no. PAPS JCPSA-104-2529-5 for 5 pages of (supplementary material). Order by PAPS number and journal reference from American Institute of Physics, Physics Auxiliary Publication Service, Carolyn Gehlbach, 500 Sunnyside Boulevard, Woodbury, NY 11797-2999. Fax: 516-576-2223, e-mail: janis@aip.org. The price is $1.50 for each microfiche (98 pages) or $5.00 for photocopies of up to 30 pages, and $0.15 for each additional page over 30 pages. Airmail additional. Make checks payable to the American Institute of Physics.

[48] W. M. Kwok and D. L. Phillips (unpublished).

[49] J. Zhang, E. J. Heller, D. Huber, D. G. Imre, and D. Tannor, J. Chem. Phys. **89**, 3602 (1988).

[50] A. B. Myers and R. A. Mathies, in *Biological Applications of Raman Spectroscopy*, edited by T. G. Spiro (Wiley, New York, 1987), Vol. 2, p. 1.

[51] A. B. Myers, in *Laser Techniques in Chemistry*, edited by A. B. Myers and T. R. Rizzo (Wiley, New York, 1995), p. 325.

[52] S. J. Riley and K. R. Wilson, Faraday Discuss. Chem. Soc. **53**, 132 (1972).

[53] W. M. Kwok and D. L. Phillips (unpublished).